MicroRNA-433 Inhibits Migration and Proliferation of Nasopharyngeal Carcinoma by Targeting Hypoxia- Induced Factor 1α

Linlin Chai
Medical School of Nantong University
Jing Cai
The People's Hospital of Rugao，Nantong
Bo You
Affiliated Hospital of Nantong University
Qicheng Zhang
Affiliated Hospital of Nantong University
Miao Gu
Affiliated Hospital of Nantong University
Ying Shan
Affiliated Hospital of Nantong University
Jie Zhang (tdfyzj@163.com)
Affiliated Hospital of Nantong University

Research Article

Keywords: miR-433, Nasopharyngeal carcinoma, hypoxia, proliferation, migration

Posted Date: May 13th, 2022

DOI: https://doi.org/10.21203/rs.3.rs-1635470/v1

Abstract

Background

Nasopharyngeal carcinoma (NPC) is a malignancy of head and neck cancer. miR-433 was downregulated in various of cancers. However, the roles and underlying mechanisms of miR-433 in the hypoxic microenvironment of NPC have not been clarified.

Methods

Real-time quantitative PCR, Western blot assay were performed to examine miR-433 and hypoxia-inducible factor-1α (HIF-1α) levels in NPC tissue and cells. Cell proliferation, migration of differentially expressed miR-433 cells was measured by Cell Counting Kit-8, Transwell analysis in vitro. Nude mice and zebrafish model were used to confirm the effect of miR-433 in vivo. Luciferase reporter assays was used to determine whether HIF-1α was a direct target of miR-433.

Results

RT-qPCR, Western blot assay were performed to show that miR-433 was down-regulated while hypoxia-inducible factor-1α (HIF-1α) was overexpressed in NPC. Cell proliferation, migration of differentially expressed miR-433 cells was measured by CCK8, Transwell analysis in vitro. Our data showed that miR-433 suppressed proliferation and migration of hypoxic NPC cells by directly binding the 3'-untranslated region (UTR) of HIF-1α. Knockdown the expression of HIF-1α in the miR-433 inhibitor treated hypoxic CNE2 cells partially reversed the effect. Nude mice and zebrafish model were used to confirm the effect of miR-433 in vivo. Luciferase reporter assays was used to determine whether HIF-1α was a direct target of miR-433.

Conclusions

NPC cells proliferation, migration, cell cycle arrest, colony formation, and the epithelial mesenchymal transition (EMT) progression were all inhibited by miR-433 by directly targeting HIF-1α. miR-433 could act as cancer suppressor miRNA and represent an effective therapeutic strategy for NPC.

Background

Nasopharyngeal carcinoma (NPC) is a common malignant tumor of the head and neck with poor prognosis [1]which cause the main death among all head and neck cancers with 60,600 incidences and 34,100 deaths in 2015 especially in Southern China [2, 3]. At first diagnosis, NPC patients often present with advanced stages and the progression-free survival is only 6 months[3]. Despite of the developments

of the radiotherapy, survival of advanced NPC patients is still poor because of recurrence, locoregional failure distant metastasis. Researches have concentrate on molecular defects including the dysregulation of miRNAs[4, 5]. miRNAs have been shown to regulate the progression of NPC by targeting specific mRNAs, such as miR-449b-5p [6], miR-205[7, 8], miR-31-5p[8] have been shown to be a potential diagnostic biomarker in NPC.

microRNAs (miRNAs) are small non-coding RNAs with an average length of 20–22 nucleotides. miRNA partially or completely complementing the 3'-untranslated region (UTR) of target genes[3] and triggers either mRNA degradation or inhibition of translation[9]. miRNA is involved in numerous biological cellular processes including proliferation, metastasis, apoptosis[10–12]. Some miRNAs are down-regulated in hypoxic cells[13, 14].

The hypoxic microenvironment is one of the major features of solid tumors and is strongly associated with poor prognosis of NPC[15]. Hypoxia-inducible factor-1α (HIF-1α) mediated tumor cells to adapt to hypoxic condition. HIF-1α accelerates the abnormal angiogenesis, metastasis, invasion of tumors [16].

Various studies have determined that miR-433 is downregulated in various of cancers such as cervical cancer[17], gastric carcinoma[18, 19], hepatocellular carcinoma[20, 21]. Aberrantly expressed miR-433 suppresses cell proliferation, differentiation, invasion[22], and is responsible for 5-fluorouracil sensitivity[23] indicating that it plays a tumor-suppressive role in normal tissues. A cohort of cancer pathways related genes has been identified and validated as targeted genes of miR-433, such as, AKT3[24], GRB2[25], Homeobox A1[26], PDCD4[27]. However, the etiopathological role of miR-433 in NPC remains largely unknown.

In the present study, the potential role of miR-433 in regulating NPC has been investigated. We identified miR-433 was downregulated in NPC cell lines and clinical tissues. HIF-1α was verified as a novel direct target of miR-433 participates in NPC cell growth and migration. Thus, this newly established miR-433/HIF-1α axis plays a key role in NPC proliferation and migration and represents a novel prognostic and therapeutic strategy for NPC.

Material And Methods

Cell culture and treatment

The NPC cell line CNE2 and the human immortalized nasopharyngeal epithelial cell line NP69 were accepted from Sun Yat-Sen University (Guangzhou, China) as gifts. The NPC cell lines (CNE1, 5-8F, 6-10B) were gifts from the Xiangya School of Medicine, Central South University. NP69 cells were cultured in serum-free medium. The four human NPC cell lines (CNE-1, CNE-2, 5-8F, 6-10B) were cultured in RPMI 1640 medium with 10% FBS (Gibco). Among them, 5-8F and 6-10B cells were cultured in complete medium with 100 U/mLpenicillin, 100 μg/mL streptomycin (Shanghai Genebase Gen-Tech Co., Ltd., Shanghai, China). All of these cell lines were incubated at 37 ° C in a humidified atmosphere

containing 5% CO_2 . In the hypoxic experiments, cells were placed in an anoxic model incubator (Billups-Rothenberg) maintained in an atmosphere of 1% O_2 , 5% CO_2 and 94% N_2 .

Statement of Ethics

The experiment was conducted with the true understanding and written consent of each patient who have been performed with the appropriate participants' informed consent in compliance with the Helsinki Declaration. All fresh primary NPC specimens with paired nasopharyngeal epithelial samples were obtained from Nantong University Affiliated Hospital(2019-L065). All patients did not receive any anti-tumor treatment prior to biopsy. All patients were confirmed by histopathology. All experiments conducted were endorsed by the Academic Committee of Nantong University. All animal experiments were ethically approved by the Jiangsu Provincial Laboratory Animal Management Committee and followed the NIH guidelines.

Cell Transfection

miR-433 mimic/ mimics NC/inhibitor/ inhibitor NC (Shanghai,China) at a final concentration of 30 nM were transfected into cells (1 x 10^5 / well) using Lipofectamine 2000 (Invitrogen) according to the manufacturer's instructions. Hs-miR-433 mimic: 5'-AUCAUGAUGGGCUCCUCGGUGU-3'. Hs-miR-433 inhibitor: ACACCGAGGAGCCCAUCAUGAU. The same method as mentioned above was used for the PEGFP-shHif-1α expression vector and the PEGFP-shRNA-NC expression vector (GeneChem, China). After 24 hours of transfection, cells were harvested and subjected to further analysis.

Western blot analysis

Western blot analysis was carried out as described previously. The antibodies used were as follows: anti-HIF-1α (Abcam; 1: 2,000 dilution), β-actin (Santa Cruz Biotechnology, CA, USA, 1: 2,000 dilution), Vimentin, E-cadherin, N-cadherin, P65,p-P65 (Cell Signaling Technology, Danvers, MA, USA, 1: 1,000 dilution). Membranes were washed, then incubated with goat anti-rabbit horseradish peroxidase-conjugated antibody (Santa Cruz Biotechnology; 1: 1,000 dilution).Blots were then developed by enhanced chemiluminescence (ECL; Cell Signaling Technology).

RT-qPCR

According to the manufacturer's instructions, 1 ml of Trizol (Invitrogen) was added to the tissues and cells, and total RNA was extracted by homogenization on ice. The real-time PCR system was subjected to real-time quantitative PCR (RT-qPCR) and SYBR Green PCR master mix (Thermo Fisher) for miRNA and mRNA analysis. The relative expression of miRNA was normalized against U6 RNA and mRNA expression was normalize using GAPDH, respectively.

Dual Luciferase Reporter Assay

To study the regulation of target genes by microRNAs, bioinformatics methods to predict potential target genes and intervention site sequences of miR-433, and design appropriate microRNA plasmids or intervention fragments, and construct reporter plasmids of target genes. Then, 293 cells (or other cells of interest) were cultured and seeded in a 12-well plate and grown for 24 hours. The reporter plasmid was co-transfected with the miR-433 binding sequence. The harvested cells are added to a specific luciferase substrate, and the luciferase reacts with the substrate to produce fluorescein, and the activity of the luciferase is determined by measuring the intensity of the fluorescence.

Cell viability assay

Cell viability was determined over time via Cell Counting Kit-8 (Beyotime Institute of Biotechnology, Shanghai, China). Cells were dissociated and seeded in 96-well plates (5×10^3 cells/well) and the plates were pre-incubated in an incubator for a suitable time (37 ° C, 5% CO_2). 10 μl of CCK8 solution was added to each well(100 μl medium), and plates were returned to the incubator for 1-4 hours. The absorbance at 450 nm was measured by using a microplate reader.

Transwell Assay

Briefly, 5×10^4 cells were mixed and transfected with serum-free DMEM, placed in the upper chamber of a 24-well Boyden Chamber (Millipore, 8-μm pore size), and 500 μl containing 10% FBS in the lower chamber. Medium. The plates were placed in an anoxic modular incubator (Billups-Rothenberg). After culturing for a suitable period of time, the chamber was taken out, fixed by methanol for 30 minutes, and crystal violet stained for 30 minutes. The upper layer of unmigrated cells was gently wiped off with a cotton swab; and washed 3 times with PBS. All migrated cells were counted using a microscope.

Flow cytometry

Cells were transfected in 6-well plates for 24 hours under hypoxic conditions. 1×10^6 transfected cells were harvested and fixed in 70% ethanol at 4 °C overnight. Wash cells 3 times with washed phosphate buffered saline (PBS), and the cells were stained in PI (BD Biosciences, Oxford, UK) staining solution in the presence of DNase without DNase in the dark. After incubation for 30 minutes in the dark at room temperature, cells were assayed by flow cytometry using cell quest software (BD FACS Aria).

Immunohistochemistry

The expression of EMT markers, ki67 and HIF-1α in NPC was analyzed by immunohistochemistry using DBA Assay Kit (ZSGB, China). Antibody drops were incubated on sections: anti-E-cadherin/N-cadherin/vimentin (1:100, CST, USA), anti-ki67 (1:100, Abcam, USA), anti-HIF-1α (1:100, Abcam, USA). Each experimental group was observed under a microscope (Leica, Wetzlar, Germany).

Quantitative analysis of serum HIF-1α expression levels

The concentration of HIF-1α in the serum samples of NPC patients was quantitatively analyzed using an enzyme-linked immunosorbent assay (ELISA) (HIF-1α ELISA kit, CSB-E12112h, CUSABIO) according to the kit instructions. About 100 μL of the standard control sample and the serum sample were added to a microtiter plate coated with HIF-1α antibody, followed by incubation for 2 hours at 37 ° C. Finally, absorbance can be measured at 450 nm and analyzed by the following method: Curve Expert.

Zebrafish transfer model

Nasopharyngeal carcinoma cells were injected into zebrafish, nasopharyngeal carcinoma cells were stained (2 g/ml of DiI, 30 min), 100-500/5 μl suspended in minimal medium, and injected into F1 zebrafish embryo (48h) yolk sac. After 48h, the cell mass transfer in zebrafish was observed by fluorescence microscope and statistical analysis was performed.

Xenograft

All BALB/c at hymic nude mice (5-6 weeks old) were provided by Shanghai Laboratory Animal Center, China, and kept in a specific pathogen-free environment. All mouse experiments followed institutional guidelines. CNE2 cells (1×10^6) in 0.1 ml 1640 medium without fetal bovine serum were subcutaneously injected into the mice. After 24 days, tumors were resected and measured for volumes.

Statistical analysis

Each experiment was repeated three times. Statistical analysis using Prism6 and SPSS 19.0 software for statistical analysis.The t test was used for comparison between groups. Data are expressed as mean ± standard deviation; $P < 0.05$ is considered statistically significant.

Results

miR-433 was downregulated in NPC tissues and cell lines

Numerous studies have suggested tumor suppressor functions of miR-433 in different malignancies[11, 22, 28]. To further substantiate a role of miR-433 involved in cancer development, we first analyzed the relevant data in The Cancer Genome Atlas (TCGA) library (https://www.cbioportal.org). According to the database, miR-433 has been recognized to be deregulated in head and neck squamous cell cancers (HNSC) (**Fig. 1a**). As NPC is the most common head and neck cancer, we further explored the expression level and the clinic-pathological significance of miR-433 in NPC. We found miR-433 was markedly down-regulated in 10 freshly-frozen NPC tissues compared with normal nasopharyngeal epithelial tissue samples (**Fig. 1b**). Consistent with this result, miR-433 down-regulated in serum samples of NPC (**Fig. 1c**). As pointed out in **Fig. 1d**, miR-433 expression was significantly decreased in NPC cell lines (CNE1, CNE2, 5-8F, 6-10B) compared to the normal nasopharyngeal cell line (NP69). Notably, CNE2 cells expressed much lower miR-433 levels. Therefore, CNE2 cells were chosen to further studied the effect of miR-433 on

NPC progression. Taken together, above data suggested that the expression levels of miR-433 were downregulated in NPC tissues and cell lines.

To further explore the role of miR-433 on the malignant phenotypes of NPC cell, we constructed both miR-433 overexpression and knockdown cell lines using lentiviral-based approaches. As indicated in **Fig.1e-g**, microscopy image showing the cells were infected with lentivirus **(Fig. 1g**), RT-qPCR results showed the expression of miR-433 was upregulated ~3.79-fold (**Fig. 1e**) in miR-433 mimic treated CNE2 cells and decreased to nearly 86% (**Fig. 1f**) in miR-433 inhibitor treated CNE2 cells.

miR-433 inbibiting NPC cell proliferation and induced cell cycle arrest in vitro

We performed the CCK-8 assay with CNE2 cells. Overexpressed miR-433 remarkably inhibited the proliferation of CNE2 cells, whereas knockdown of miR-433 enhanced the growth of CNE2 cells significantly (**Fig. 2a-b**). We presumed that miR-433 affected cell cycle progression of NPC cells. miR-433 overexpression induced G1-phase arrest determined by flow cytometry analysis. miR-433 knockdown antagonized this effect of miR-433 overexpression (**Fig. 2c-d**). Colony formation assays showed that compromised colony-forming ability of CNE2 cells transfected with miR-433 lentivirus, whereas compared with control cells, miR-433 knockdown promoted cell growth (**Fig. 2e-f**). Dates above supported the finding that ectopic expression of miR-433 exerted tumor suppressor function by inhibiting NPC cell proliferation, inducing cell cycle arrest.

Many researchers indicated that activated NF-κB signaling has been shown associated with several aspects of tumorigenesis such as angiogenesis, metastasis, anti-apoptosis and therapy resistance[29]. As shown in **Fig. 2g** , the active expression levels of NF-κB were decreased in the miR-433 mimic treated CNE2 cells, whereas the protein levels of activated NF-κB were significantly increased in CNE2-miR-433-inhibitor cells. These results demonstrated that miR-433 regulated the NF-κB signaling pathway in NPC.

miR-433 Negatively Regulated CNE2 Migration in vitro and in vivo

Transwell migration assays showed that miR-433 mimic transfected CNE2 cells strikingly decreased the migration capacity, which markedly increased in miR-433 inhibitor treated CNE2 cells (**Fig. 3a-b**). Based on this, we speculated that miR-433 may participate in the process of EMT.As showed in **Fig, 3c,** miR-433 mimic increased the E- cadherin level, which acts as an epithelial cell marker.As the same time, the level of the mesenchymal marker N-cadherin and Vimentin was down-regulated. Dil-labeled CNE2 cells with different miR-433 expression levels were injected at the blastula stage to explore the potential effect of miR-433 on CNE2 cells metastases in vivo. After implantation for 8 days, more miR-433 inhibitor treated CNE2 cells were disseminated away from primary sites (**Fig. 3d-e**). These findings emphasize that miR-433 negatively regulates cell migration.

HIF-1α was a Direct Target of miR-433

In order to distinguish the molecular mechanisms responsible for the effect of miR-433 observed above, the online bioinformatic analysis were employed to identify potential miR-433 target genes (**Fig. 4a**). Bioinformatics analysis (TargetScan, miRDB, DIANA) revealed that HIF-1α was predicted by databases mentioned above. HIF-1α lays a central role in the metastatic process of NPC. We came up with an assumption that miR-433 may inhibit the progression of NPC by directly targeting HIF-1α. We then analyzed the expression of HIF-1α in NPC. As showed in **Fig. 4b,** HIF-1α was overexpressed in the serum of NPC patients. We next measured the expression levels of HIF-1α in human NPC samples by immunochemistry and Western blot analysis. We analyzed HIF-1α expression in NPC tissues and normal tissues using immunochemistry. The results showed that the expression level of HIF-1α was overexpressed in NPC samples which was mainly localized to the nuclei (**Fig. 4c**). Western blot results were further confirmed the result that HIF-1α was over-expressed in NPC tissues (**Fig. 4d-e**). As indicated in **Fig. 4f**, HIF-1α protein expression level was higher in hypoxic CNE2 and 5-8F compared to the normoxic cells. In addition, after incubating NPC cells under oxygen deprivation conditions, Western blot analysis showed that the protein expression of HIF-1α increased with a time dependency (**Fig. 4g-h**). As **Fig. 4i-j** showed, after exposing cells to $CoCl_2$ in serum-free medium under normal conditions to mimic hypoxic conditions, HIF-1α up-regulated with a concentration dependency.

To further confirm the conjecture that miR-433 functions by directly targeting HIF-1α, we investigated the influence of mutative miR-433 level on the expression of HIF-1α under hypoxia conditions.

After transfection of miR-433 mimic or miR-433 inhibitor, the HIF-1α protein level was altered in hypoxic CNE2 cells, changes of which were determined by Western blot analysis(**Fig. 4k**). The cellular immunofluorescence data showed that HIF-1α levels, under hypoxia, were consistently down-regulated in miR-433 mimic treated CNE2 cell lines while miR-433 inhibitor resulted in the opposite results (**Fig. 4l**). HIF-1α expression was attenuated in CNE2 cells after transfected with miR-433 mimic as well as been promoted after miR-433 inhibitor transfection (**Fig. 4k-l**). As bioinformatics analysis indicated that the 3'-UTR of HIF-1α contained a predicted binding site for miR-433 (**Fig. 4m**), a luciferase reporter assay was then carried out. Results showed that miR-433 inhibited the luciferase activity of the WT 3'-UTR of HIF-1α (**Fig. 4n**) which indicated that HIF-1α was a direct target of miR-433.

HIF-1α ameliorates the inhibitory effect of miR-433 on NPC progression

To further confirm the hypothesis that miR-433 regulated NPC progression through directly targeting HIF-1α, miR-433 inhibitor treated CNE2 cells were then transfected with sh-HIF-1α under hypoxic conditions. HIF-1α knockdown was verified byWestern blotting analysis (**Fig. 5a**). The ectopic expression of HIF-1α rescued miR-433-mediated migration and proliferation of CNE2 cells (**Fig. 5b-c**). According to the results of CCK-8 assays, knockdown of the expression of HIF-1α increased the inhibitory effects of miR-433 on cell proliferation significantly (**Fig. 5b**). Moreover, suppressed migration of hypoxic CNE2 cells were accelerate by knockdown of HIF-1α (**Fig. 5c**). In a word, results above confirmed that the miR-433/ HIF-1α axis played an important role in proliferation process as well as in cell migration ability of NPC cells.

miR-433 inhibits xenograft tumor growth in vivo

To further explore the impact of miR-433 on tumor growth in vivo, xenograft animal model was set up by implanting the CNE2 cells with stable overexpression and knockdown of miR-433 into nude mice. Every four days, each mouse was monitored. Compared with tumors derived from miR-433-NC transfected CNE2 cell, stable over-expressed miR-433 treated CNE2 cells result in the decrease in tumor volume (**Fig. 6a-b**). Significantly larger average tumor volume was in miR-433-inhibitor treated cells than that in control mice, at the same time, tumors were also heavier (**Fig. 6c-d**).

Moreover, RT-qPCR analysis was shown in **Fig. 6e**, miR-433 level was increased in the miR-433 mimic transfected group, while decreased in miR-433 inhibitor treated group. HIF-1α expression was decreased in the miR-433 mimic treated group, as elevated HIF-1α expression was in miR-433-inhibitor- transfected group (**Fig. 6f**). As shown in **Fig. 6f**, Ki-67 staining of the xenograft tumors was further confirming the suppressing effect of miR-433 on NPC proliferation. Immunohistochemistry (**Fig. 6f)**Western blot(**Fig. 6j)** and RT-qPCR (**Fig. 6g-i)** analyzed the expression of E-cadherin, N-cadherin, Vimentin which was further confirmed the inhibitory effect of miR-433 on EMT. In vitro studies revealed that miR-433 suppressed NPC tumor growth by repressing HIF-1α expression and EMT.

Discussion

In this study, for the first time, we identified miR-433 was a tumor suppressor in NPC. miR-433 suppressed the metastasis and proliferation in NPC. NF-κB signaling pathway was also regulated by miR-433. Bioinformatics analysis and luciferase reporter assays were used to validate HIF-1α as a direct target of miR-433. Overexpression or knockdown of miR-433 in hypoxic CNE2 cells responsively modified the expression levels of HIF-1α. Furthermore, knockdown the expression of HIF-1α arrested the stimulatory impact of miR-433 inhibitor. Our data demonstrated that miR-433 acts as a tumor- suppressor by inhibiting CNE2 cell proliferation, colony formation, migration in vitro and by slowing in vivo tumor growth.

HIF-1α accumulated under hypoxic condition. HIF-1α plays an essential mediator of cellular response to hypoxia including drug resistance, metastasis, tumor proliferation, differentiation and radio-resistance as well as in NPC. As we previously showed that HIF-1α overexpression is associated with poor prognosis in NPC patients[30]. In presented research, we showed that, hypoxic NPC cells exhibited enhanced migration and proliferation capability, which was suppressed by miR-433 in NPC cells.

miRNAs play as important regulators in tumorigenesis and microenvironment reprogramming. Oncogenic or tumor-suppressive effect in cancer pathogenesis were detailed elucidated which may help us identify effective biomarkers for cancer diagnosis and prognosis as well as therapeutic targets. Numerous studies reported the dysregulation of miRNAs have differential effects on NPC[31]. miR-433 is located at 14q32 (miRBase, http:microrna.sanger.ac.uk/) in humans, a region that is often involved in several types of translocations in hematological malignancies. Abnormal expression of miR-433 was reported in

variety types of human cancer. Downregulation of miR-433 was observed in cervical cancer[17], gastric carcinoma[18, 19], hepatocellular carcinoma[20, 21]. miR-433 directly targeted metadherin to regulate the β-catenin and AKT signaling pathways which inhibited cervical cancer progression [17]. miR-433 inhibits breast cancer cell growth via the MAPK signaling pathway by targeting Rap1a[28].These studies elucidated that miR-433 might perform an important role in many types of tumor and might be further investigated as a potential therapeutic target for the treatment.

In the present work, our data showed that miR-433 was down-regulated in NPC tissues and cell lines compared with normal controls. miR-433 overexpression suppressed NPC cell proliferation and migration in vitro and reduced tumor growth in vivo. HIF-1α was predicted as a potential target of miR-433 using bioinformatics analysis which was overexpressed in NPC. Western blot analysis and RT-qPCR results revealed that miR-433 negatively regulated HIF-1α expression at protein levels in NPC cells under hypoxia conditions. Subsequently, bioinformatics analysis indicated the direct binding site of miR-433 to HIF-1α 3'-UTR. Then, the luciferase reporter assays further confirmed the direct function relation between miR-433 and HIF-1α. Our experimental data further revealed that HIF-1α knockdown showed tumor-suppressive roles similar to miR-433 overexpression in NPC.

Conclusions

In summary, our findings support that miR-433 can attenuate the expression of HIF-1α and regulate the proliferation and migration of NPC. Our dates will help to further understand the function and mechanism of miRNAs in NPC. miR-433 may be employed as therapeutic for NPC. Taken together, our data provide new mechanistic insights into possible signaling pathways involved in maintaining proliferation and migration of NPC cells.

Abbreviations

HIF-1α：hypoxia-inducible factor-1α; EMT：epithelial mesenchymal transition; HNSC : head and neck squamous cell cancers.

Declarations

Ethics approval and consent to participate

The authors are accountable for all aspects of the work in ensuring that questions related to the accuracy or integrity of any part of the work are appropriately investigated and resolved. All procedures performed in this study involving human participants were in accordance with the Declaration of Helsinki (as revised in 2013). The study was approved by Nantong University Affiliated Hospital(2019-L065). Experiments were performed under a project license (NO.:20190304-005) granted by Academic Committee of Nantong University, in compliance with the Jiangsu Provincial Laboratory Animal Management Committee national or institutional guidelines for the care and use of animals

Consent for Publication

Not applicable.

Availability of Data and Materials

The datasets supporting the conclusions of this article are included within the article

Competing interests

The authors declare that there is no conflict of interest.

Funding

This work was supported by grants from the National Natural Science Foundation of China (Grant No.82103435).

Authors' contributions

JZ and YS designed the study, reviewed the manuscript and guaranteed the integrity of the whole study. LLC and JC carried out the whole experiments and drafted the manuscript. BY, QCZ and MG analyzed the data and literature reports. The author(s) read and approved the final manuscript.

Acknowledgements

This work was supported by grants from the National Natural Science Foundation of China (Grant No.82103435)

Author details

[1]Departments of Otorhinolaryngology, Medical School of Nantong University, Nantong, China

[2]Department of Otorhinolaryngology Head and Neck surgery,The People's Hospital of Rugao Nantong, China

[3]Department of Otorhinolaryngology Head and Neck surgery, Affiliated Hospital of Nantong University, Nantong, China

References

1. Zheng ZQ, Li ZX, Zhou GQ, Lin L, Zhang LL, Lv JW, Huang XD, Liu RQ, Chen F, He XJ, Kou J, Zhang J, Wen X, Li YQ, Ma J, Liu N, Sun Y. Long non-coding RNA FAM225A promotes nasopharyngeal carcinoma tumorigenesis and metastasis by acting as ceRNA to sponge miR-590-3p/miR-1275 and upregulate ITGB3. Cancer Res 2019.

2. Chua MLK, Wee JTS, Hui EP, Chan ATC. Nasopharyngeal carcinoma. Lancet 2016, **387**(10022): 1012–1024.
3. Li Y, He Q, Wen X, Hong X, Yang X, Tang X, Zhang P, Lei Y, Sun Y, Zhang J, Wang Y, Ma J, Liu N. EZH2-DNMT1-mediated epigenetic silencing of miR-142-3p promotes metastasis through targeting ZEB2 in nasopharyngeal carcinoma. Cell Death Differ 2019, **26**(6): 1089–1106.
4. Zhao S, Jie C, Xu P, Diao Y. MicroRNA-140 inhibit prostate cancer cell invasion and migration by targeting YES proto-oncogene 1. J Cell Biochem 2019.
5. Ghaemi Z, Soltani BM, Mowla SJ. MicroRNA-326 Functions as a Tumor Suppressor in Breast Cancer by Targeting ErbB/PI3K Signaling Pathway. Front Oncol 2019, **9**: 653.
6. Yin W, Shi L, Mao Y. MicroRNA-449b-5p suppresses cell proliferation, migration and invasion by targeting TPD52 in nasopharyngeal carcinoma. J Biochem 2019.
7. Zhang P, Lu X, Shi Z, Li X, Zhang Y, Zhao S, Liu H. miR-205-5p regulates epithelial-mesenchymal transition by targeting PTEN via PI3K/AKT signaling pathway in cisplatin-resistant nasopharyngeal carcinoma cells. Gene 2019, **710**: 103–113.
8. Yi SJ, Liu P, Chen BL, Ou-Yang L, Xiong WM, Su JP. Circulating miR-31-5p may be a potential diagnostic biomarker in nasopharyngeal carcinoma. Neoplasma 2019, **2019**.
9. Zhang J, Huang T, Zhou Y, Cheng ASL, Yu J, To KF, Kang W. The oncogenic role of Epstein-Barr virus-encoded microRNAs in Epstein-Barr virus-associated gastric carcinoma. J Cell Mol Med 2018, **22**(1): 38–45.
10. Suzuki H, Maruyama R, Yamamoto E, Kai M. Epigenetic alteration and microRNA dysregulation in cancer. Front Genet 2013, **4**: 258.
11. Zhang Y, Fei M, Xue G, Zhou Q, Jia Y, Li L, Xin H, Sun S. Elevated levels of hypoxia-inducible microRNA-210 in pre-eclampsia: new insights into molecular mechanisms for the disease. J Cell Mol Med 2012, **16**(2): 249–259.
12. Yi B, Piazza GA, Su X, Xi Y. MicroRNA and cancer chemoprevention. Cancer Prev Res (Phila) 2013, **6**(5): 401–409.
13. Byun Y, Choi YC, Jeong Y, Lee G, Yoon S, Jeong Y, Yoon J, Baek K. MiR-200c downregulates HIF-1alpha and inhibits migration of lung cancer cells. Cell Mol Biol Lett 2019, **24**: 28.
14. Hua Z, Lv Q, Ye W, Wong CK, Cai G, Gu D, Ji Y, Zhao C, Wang J, Yang BB, Zhang Y. MiRNA-directed regulation of VEGF and other angiogenic factors under hypoxia. PLoS One 2006, **1**: e116.
15. Yip C, Cook GJ, Wee J, Fong KW, Tan T, Goh V. Clinical significance of hypoxia in nasopharyngeal carcinoma with a focus on existing and novel hypoxia molecular imaging. Chin Clin Oncol 2016, **5**(2): 24.
16. Zhou X, Huang D, Xue Z, Xu X, Wang K, Sun Y, Kang F. Effect of HIF-1alpha on biological activation of human tongue squamous cell carcinoma SCC-15 cells in vitro. Int J Oncol 2015, **46**(6): 2346–2354.
17. Liang C, Ding J, Yang Y, Deng L, Li X. MicroRNA-433 inhibits cervical cancer progression by directly targeting metadherin to regulate the AKT and beta-catenin signalling pathways. Oncol Rep 2017,

38(6): 3639–3649.

18. Yang O, Huang J, Lin S. Regulatory effects of miRNA on gastric cancer cells. Oncol Lett 2014, **8**(2): 651–656.
19. Guo LH, Li H, Wang F, Yu J, He JS. The Tumor Suppressor Roles of miR-433 and miR-127 in Gastric Cancer. Int J Mol Sci 2013, **14**(7): 14171–14184.
20. Xue J, Chen LZ, Li ZZ, Hu YY, Yan SP, Liu LY. MicroRNA-433 inhibits cell proliferation in hepatocellular carcinoma by targeting p21 activated kinase (PAK4). Mol Cell Biochem 2015, **399**(1–2): 77–86.
21. Yang Z, Tsuchiya H, Zhang Y, Hartnett ME, Wang L. MicroRNA-433 inhibits liver cancer cell migration by repressing the protein expression and function of cAMP response element-binding protein. J Biol Chem 2013, **288**(40): 28893–28899.
22. Zhang J, Zhang L, Zhang T, Dong XM, Zhu Y, Chen LH. Reduced miR-433 expression is associated with advanced stages and early relapse of colorectal cancer and restored miR-433 expression suppresses the migration, invasion and proliferation of tumor cells in vitro and in nude mice. Oncol Lett 2018, **15**(5): 7579–7588.
23. Gotanda K, Hirota T, Matsumoto N, Ieiri I. MicroRNA-433 negatively regulates the expression of thymidylate synthase (TYMS) responsible for 5-fluorouracil sensitivity in HeLa cells. BMC Cancer 2013, **13**: 369.
24. Hu X, Wang J, He W, Zhao P, Ye C. MicroRNA-433 targets AKT3 and inhibits cell proliferation and viability in breast cancer. Oncol Lett 2018, **15**(3): 3998–4004.
25. Shi Q, Wang Y, Mu Y, Wang X, Fan Q. MiR-433-3p Inhibits Proliferation and Invasion of Esophageal Squamous Cell Carcinoma by Targeting GRB2. Cell Physiol Biochem 2018, **46**(5): 2187–2196.
26. Li H, Li J, Yang T, Lin S, Li H. MicroRNA-433 Represses Proliferation and Invasion of Colon Cancer Cells by Targeting Homeobox A1. Oncol Res 2018, **26**(2): 315–322.
27. Sun Y, Wang F, Wang L, Jiao Z, Fang J, Li J. MicroRNA-433 regulates apoptosis by targeting PDCD4 in human osteosarcoma cells. Oncol Lett 2017, **14**(2): 2353–2358.
28. Zhang T, Jiang K, Zhu X, Zhao G, Wu H, Deng G, Qiu C. miR-433 inhibits breast cancer cell growth via the MAPK signaling pathway by targeting Rap1a. Int J Biol Sci 2018, **14**(6): 622–632.
29. Chen Y, Chen L, Yu J, Ghia EM, Choi MY, Zhang L, Zhang S, Sanchez-Lopez E, Widhopf GF, 2nd, Messer K, Rassenti LZ, Jamieson C, Kipps TJ. Cirmtuzumab Blocks Wnt5a/ROR1-Stimulation Of NF-kappaB To Repress Autocrine STAT3-Activation In Chronic Lymphocytic Leukemia. Blood 2019.
30. Shan Y, You B, Shi S, Shi W, Zhang Z, Zhang Q, Gu M, Chen J, Bao L, Liu D, You Y. Hypoxia-Induced Matrix Metalloproteinase-13 Expression in Exosomes from Nasopharyngeal Carcinoma Enhances Metastases. Cell Death Dis 2018, **9**(3): 382.
31. Jiang X, Dai B, Feng L. miR-543 promoted the cell proliferation and invasion of nasopharyngeal carcinoma by targeting the JAM-A. Hum Cell 2019.

Figures

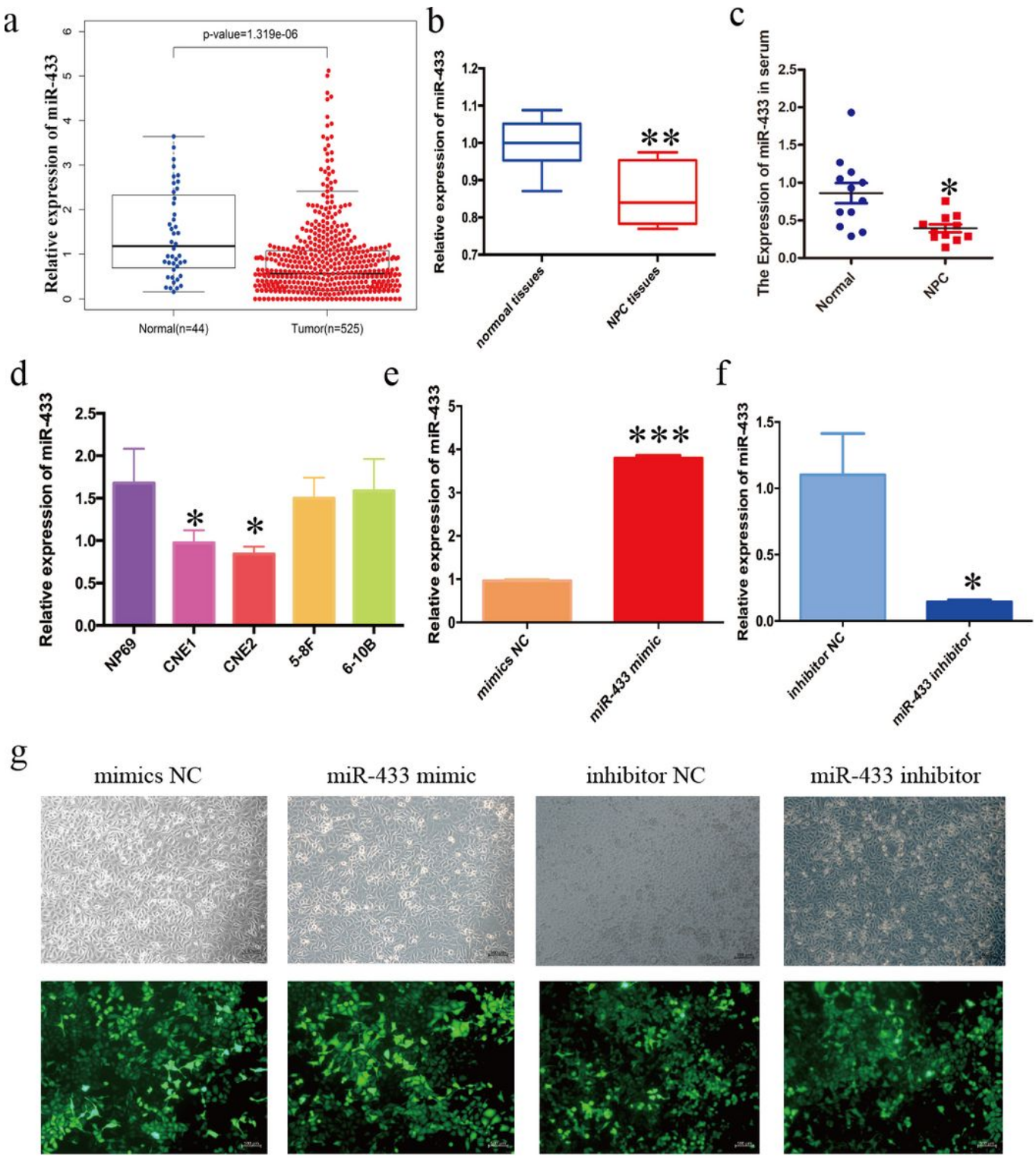

Figure 1

(a)Published data from The Cancer Genome Atlas (TCGA) library. (b) RT-qPCR examination of miR-433 levels in NPC tissues and normal tissues. (c) RT-qPCR analysis was carried out to revealed the expression of miR-433 in serum samples of NPC and normal donors. (d)The expression of miR-433 in NPC cell lines and in human immortalized nasopharyngeal epithelial cell line was tested by RT-qPCR. (e) Lentivirus overexpressing miR-433 (defined as miR-433 mimic) or (f) lentivirus with short hairpin RNA targeting miR-

433 (defined as miR-433-inhibitor) were transfected to CNE2 cells. A non-targeting sequence were used as the negative control (NC). RT-qPCR analyzed the miR-433 expression levels. (g) Representative microscopy image showing the cells were infected with lentivirus. All experiments were performed in triplicate. *$P < 0.05$, ***$P < 0.01$.

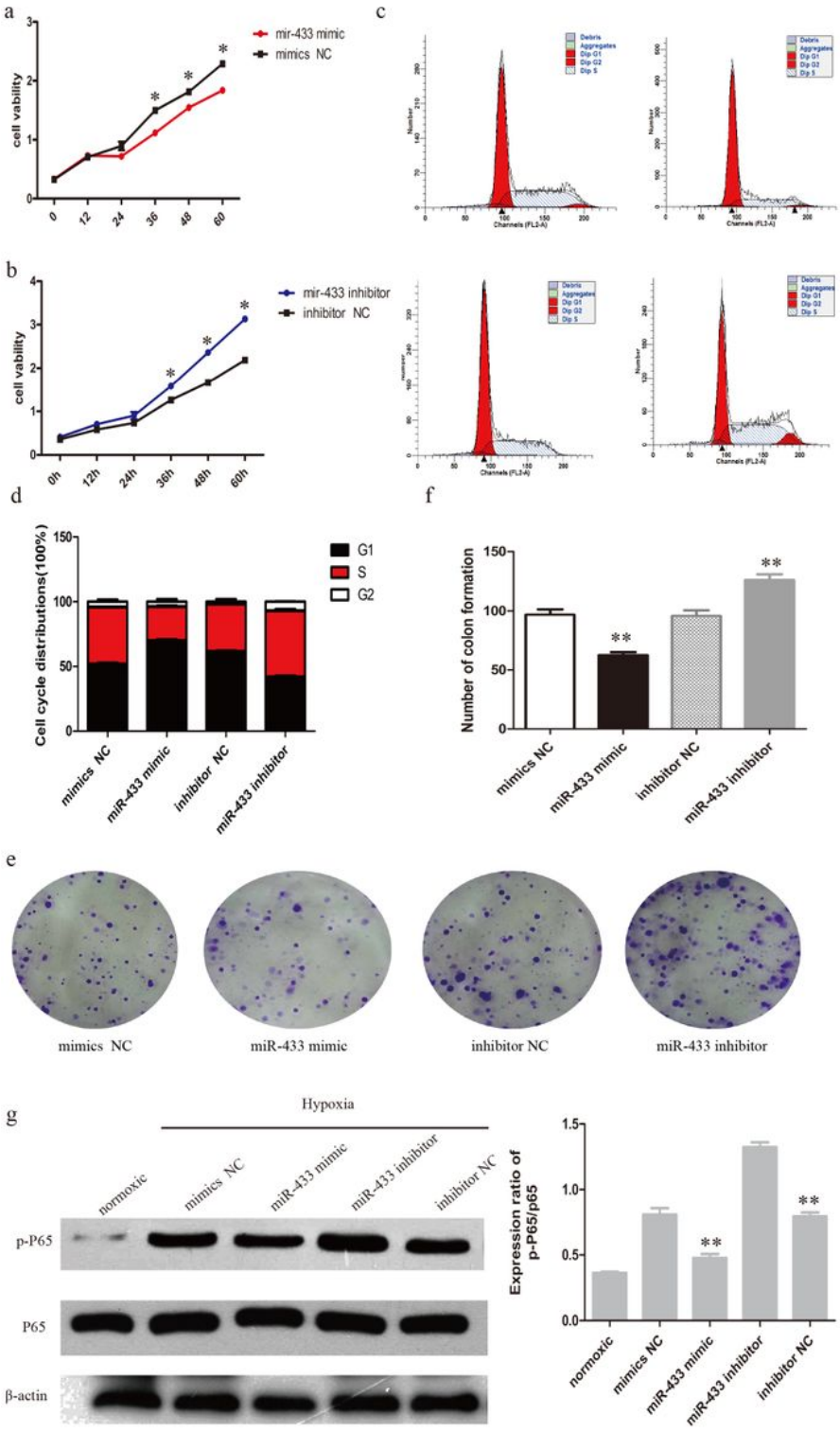

Figure 2

miR-433 suppressed NPC cell proliferation and induced cell cycle arrest

Cell proliferation ability was compared between miR-433 mimic (a) and inhibitor (b) transfected CNE2 cells by the CCK-8 assay. (c-d) Flow cytometry results showing the cell cycle distribution in miR-433 mimic and inhibitor treated CNE2 cells. (e-f) The colony formation ability of miR-433 overexpressing or silencing CNE2 cells. (g)Western blotting measure the levels of activated NF-κB, activated NF-κB and β-actin in CNE2 cells with up-regulated or down-regulated miR-433 expression. Three duplicates were performed for each group, and three independent experiments were performed. *$P < 0.05$, **$P < 0.01$. All data are represented as the means ± S.E.M

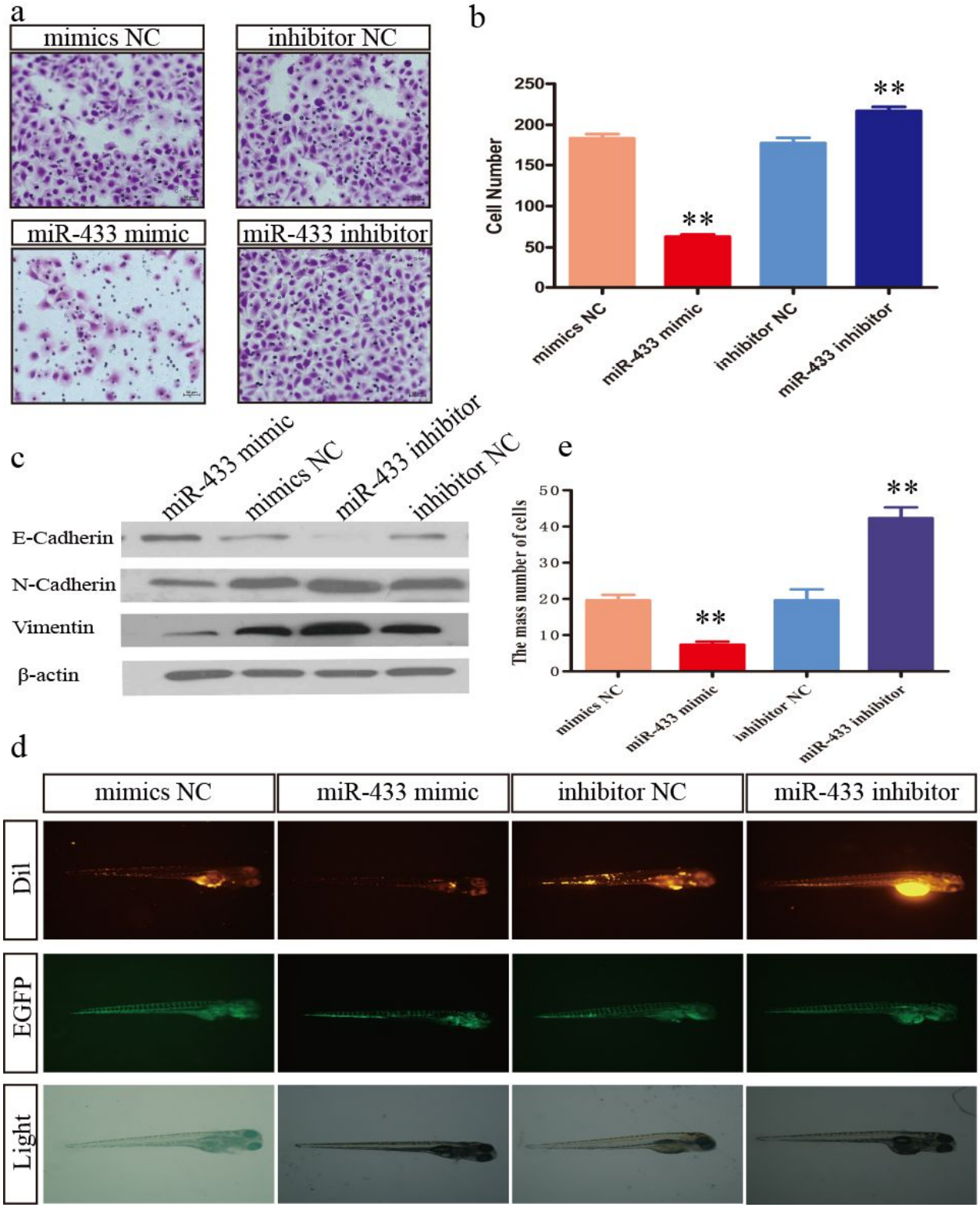

Figure 3

miR-433 Negatively Regulated CNE2 Migration in vitro and in vivo

(a) miR-433 mimic, inhibitor and the negative control were transfected to CNE2 cells. Transwell assays were used to measure the metastasis ability of each group. (b) Migratory cells were quantified. (c) Western blot analysis was set up to detect the effects of miR-433 on epithelial-mesenchymal transition

(EMT). (d) CNE2 cells were transfected with the miR-433 mimic, inhibitor or negative control. CNE2 cells labeled Dil were injected into the perivitelline space of 48 hours post fertilization zebrafish embryos. At day 8 post injection, CNE2 cell masses were detected using fluorescence microscopy. (e) The numbers of tumor foci were quantified.Data represent at least three experiments performed in triplicate, * $P < 0.05$; ** $P < 0.001$.

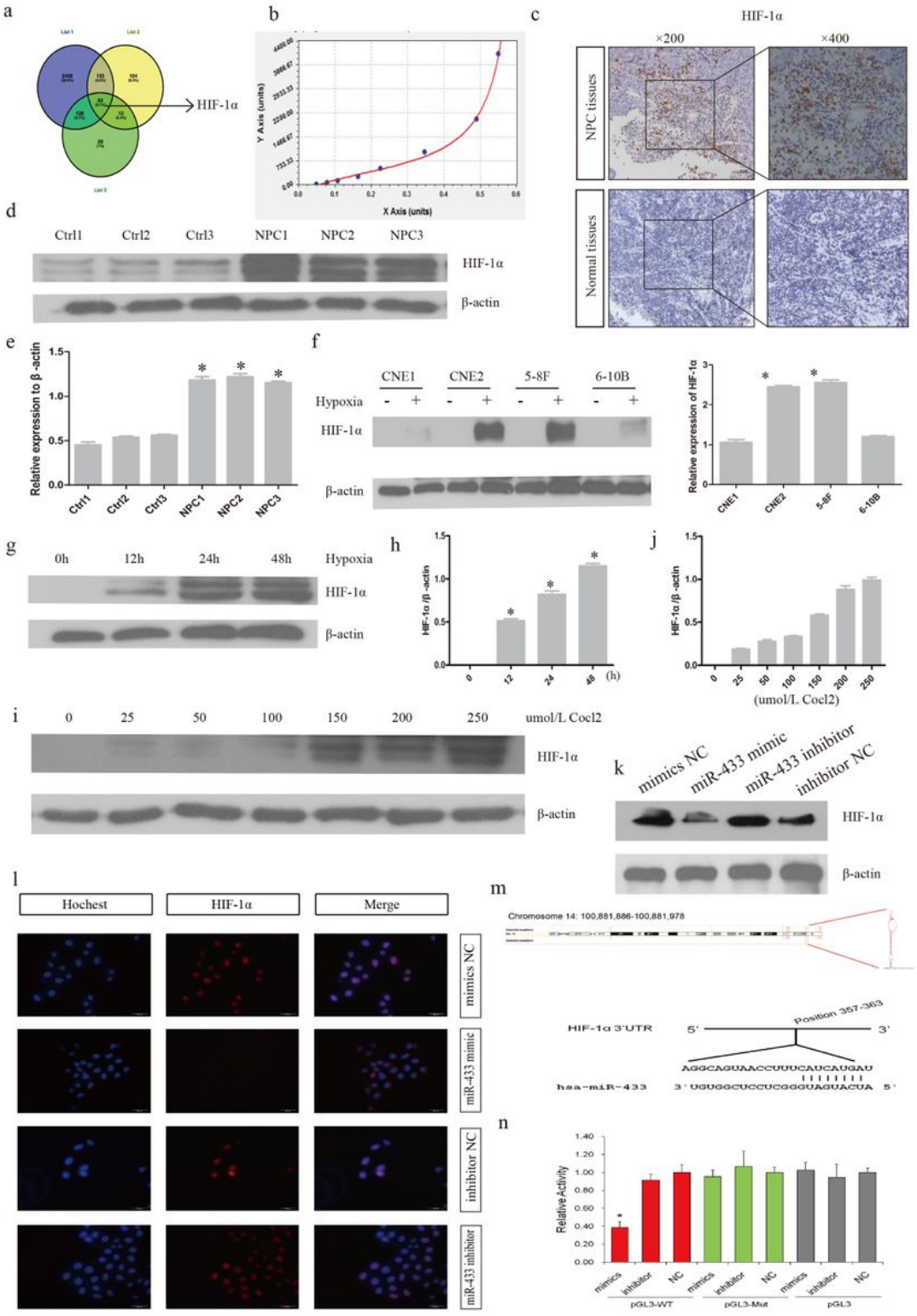

Figure 4

HIF-1α was a Direct Target of miR-433

(a) Venn diagram displaying that HIF-1α as miR-433 computationally predicted arget HIF-1α by three different prediction programs: TargetScan, miRDB, and DIANA. (b) The expression of HIF-1α in serum of NPC patients and normal donors were measured by the standardcurve analysis. (c) Immunostaining images of HIF-1α in NPC tissues and normal tissues samples. (d-e) Western blotting analysis the expression of HIF-1α in NPC samples. (f) HIF-1α protein expression levels were examined in four NPC cell lines under normoxic and hypoxic conditions. Western blot analysis of HIF-1α expression levels in the poorly differentiated CNE2 cells under normal (normorxic), hypoxic conditions (hypoxia) for 0-48hours (g-h) or after treatment with the hypoxia mimetic $CoCl_2$ with different concentration(i-j). (k) The relative protein expression of HIF-1α in hypoxic CNE2 cells treated with the miR-433 mimic or miR-NC was measured by Western blot. (l) After miR-433 transfecting, CNE2 cells were incubated under hypoxia for 24 h. Immunofluorescence staining analysis of the nuclear expression of HIF-1α (Red) in Cells. Blue is the nuclear staining by Hoechst. (m) Potential interaction between the putative binding sites in the 3'-UTR of HIF-1α and miR433. (n) Luciferase reporter assay shows miR-433 significantly suppressed the luciferase activity of the wild-type HIF-1α 3’- UTR. Qualitative changes from three independent experiments are shown as histograms. *$P < 0.05$, **$P < 0.01$ compared with cells transfected with negative control. All data are represented as the means ± S.E.M

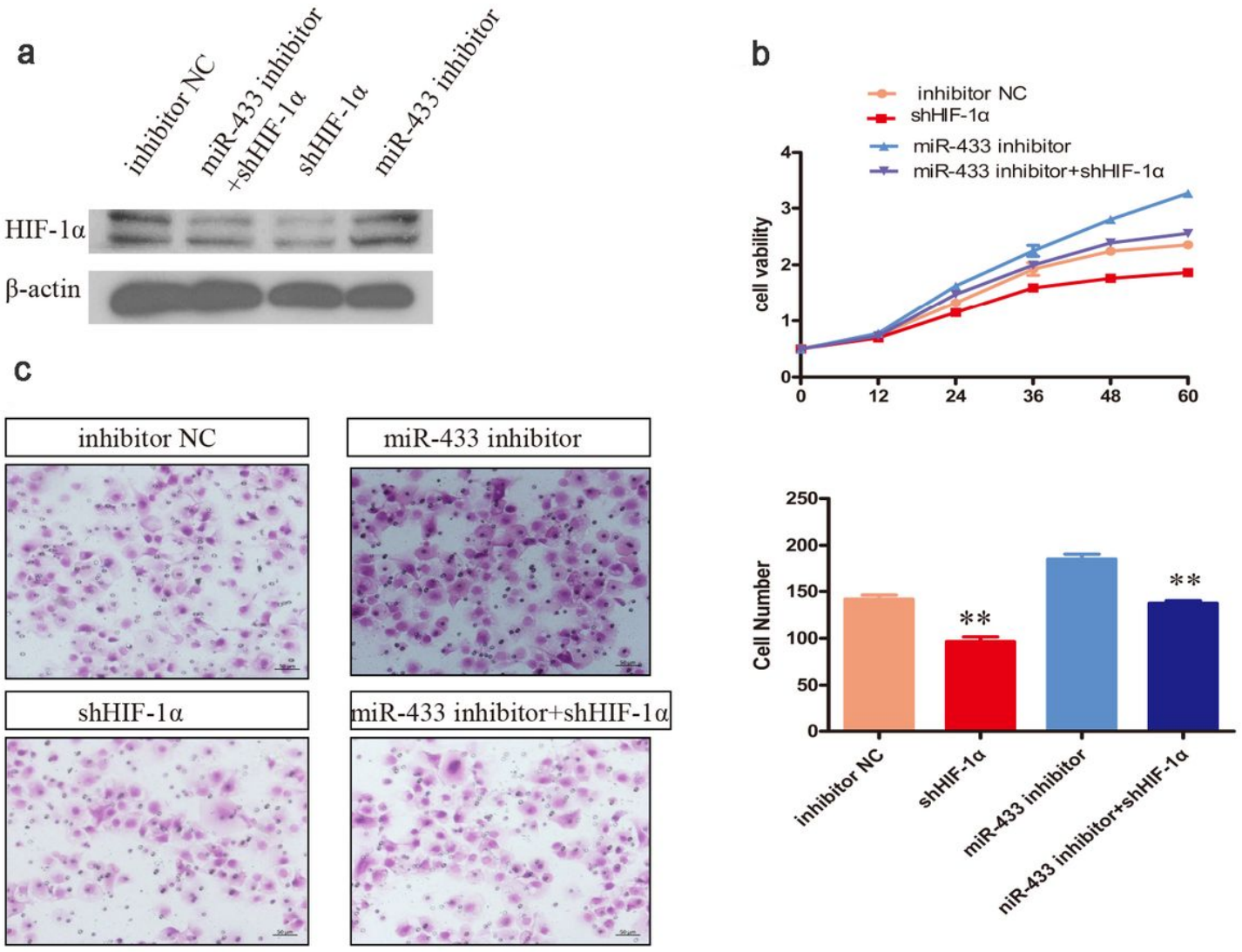

Figure 5

HIF-1α attenuates the inhibitory effect of miR-433

(a) Expression of HIF-1α in hypoxic CNE2 cells transfected with miR-433 inhibitor and HIF-1α knockdown lentivirus (sh-HIF-1α). (b) CCK-8 analysis of CNE2-miR-433 mimic cells transfected with sh-HIF1α or sh-NC. (c) Transwell assay analysis the migration ability of CNE2-miR-433 mimic cells treated with sh-HIF1α or sh-NC. Three independent experiments were performed. All data are represented as the means ± S.E.M. **P* < 0.05, ***P* < 0.01, compared with the negative control group.

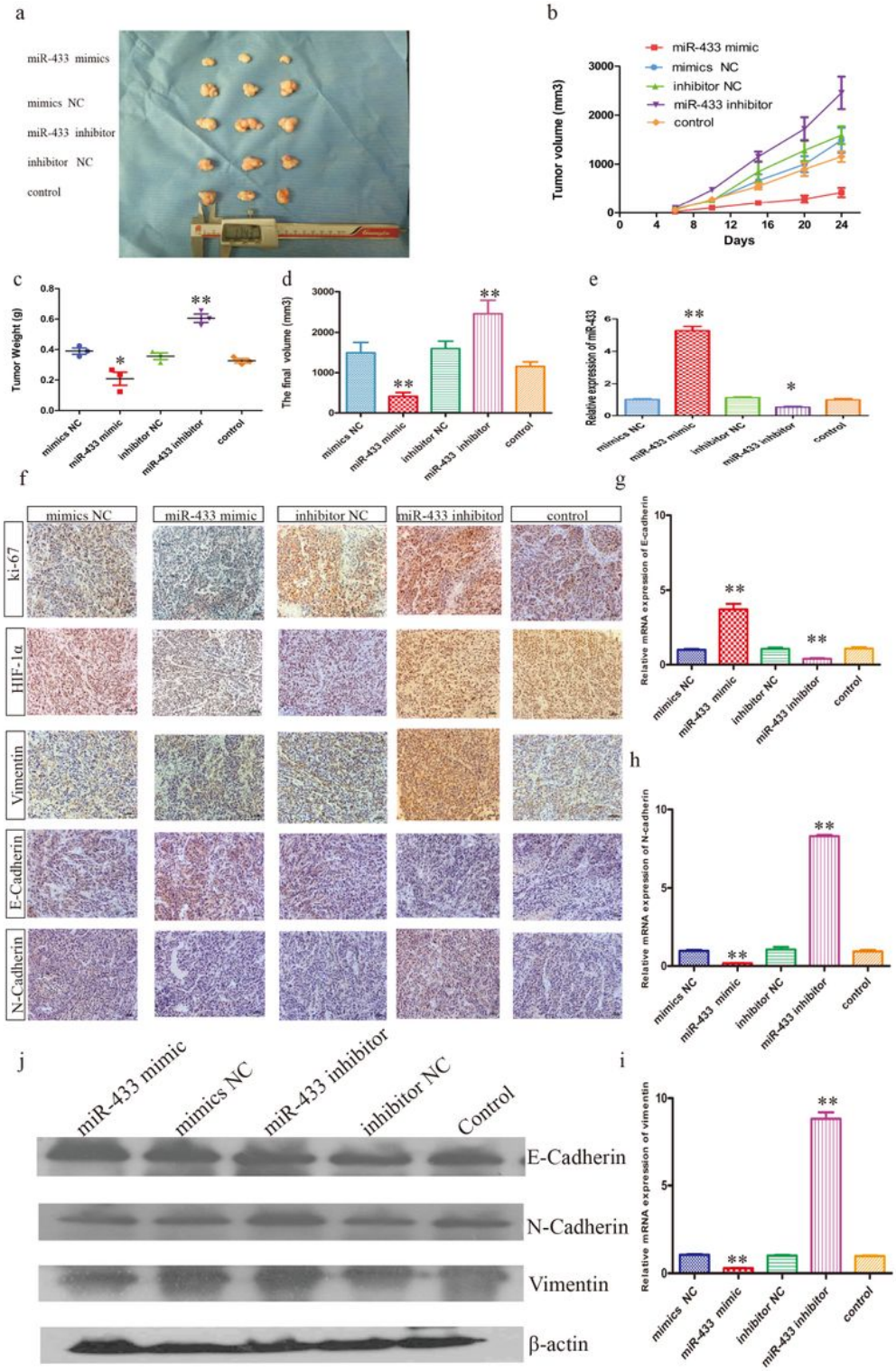

Figure 6

miR-433 suppresses xenograft tumor growth in vivo

(a) photographs and (b) growth curves of tumors derived from mice inoculated with miR-433 mimic, miR-433 mimics NC, miR-433 inhibitor, miR-433-inhibitor NC treated CNE2 cells, control CNE2 cells were used as control (n = 3 per group). Volume (mm^3) = Length (mm) × $Width^2$ (mm^2) × 0.5 was used to calculated

the tumor volume was calculated based on the following equation. (c) Tumor weight and (d) the final volume of the xenografts derived from each mouse. (e) RT-qPCR analysis was used to measure miR-433 expression levels in xenografts of each groups. (f) Immunohistochemistry measuring Ki-67, HIF-1α, Vimentin, E-cadherin and N-cadherin levels in tumors of each group. (g-i) RT-qPCR analyzed the mRNA levels of E-cadherin, Vimentin, N-cadherin in xenografts derived from mice of each group. (j) EMT-related markers determined by Western blot analysis. All data are presented as the means ± S.E.M Three independent experiments were performed for each group. *$P < 0.05$, **$P < 0.001$